Strain–Tensor Components, Crystallite Shape, and Their Effects on Crystalline Structure in Silk I

Sangappa,[1] Kenji Okuyama,[2] R. Somashekar[3]

[1]*Department of Physics, Yuvaraja's College, University of Mysore, Mysore-570 005, India*
[2]*Department of Biotechnology, Tokyo University of Agriculture and Technology, Tokyo, Japan*
[3]*Department of Studies in Physics, University of Mysore, Manasagangotri, Mysore-570 006, India*

Received 17 January 2002; accepted 8 July 2003

ABSTRACT: By using the X-ray powder data obtained from *Bombyx mori* silk fibroin in silk I modification, we have estimated the strains by using profiles of several (*hkl*) reflections observed in the fibroin. For this purpose, we have used line profile simulation and matching with the experimental, on the basis of a paracrystalline one-dimensional Hosemann's model proposed earlier. The shape of the crystallite and size along different directions in the fibroin have also been estimated and presented here. From these results, the strain tensor has been computed by using the approach given by Wilke and Martis. The effect of these strains on the molecular arrangement within the crystal structure and the nature of changes in the chain within the unit cell which participates in inducing the intrinsic strain during the formation of the fiber (*silkII*) are reported here. © 2004 Wiley Periodicals, Inc. J Appl Polym Sci 91: 3045–3053, 2004

Key words: WAXS; crystal imperfection parameters; crystal structure; strain tensor; silk I

INTRODUCTION

Silks are an intriguing class of fibrous proteins that attracts a continued interest from various investigators. Because of its extensive use in the textile industry, it is of interest to know the structure–property relationship with respect to protein folding and assembly. Three modifications of silks fibroin (I, II, and III) are observed. Silk I is observed in silk gland[1–3] and spun silk is silk II modification. Silk III modification is observed in air–water interface of silk fibroin solution.[4] The crystal and molecular structure of silk II are given by Marsh et al.,[5] and the structure of silk III was given by Valluzzi et al.[4] Recently, refined molecular and crystal structure of silk I based on dipeptide and hexapeptide were reported by Okuyama et al.[6] The broadening of X-ray reflection profiles in spun silk (II) fibers in terms of crystal size and strain have been studied extensively[7–13] by using Hosemann's one-dimensional paracrystalline model. In fact, a similar paracrystalline type of broadening was observed during the investigations of silk I.[6] In this article, we report the percentage of lattice distortion along different directions in the fiber by using Warren's Fourier method,[14,15] and hence, a procedure has been given to estimate the strain tensor components of silk I modification. Also, the shape of the crystallite in silk I has been computed by using these results. Further, for the first time, we have used strain-corrected integrated intensities of various reflections to obtain the molecular and crystal structure of the silk I modification, and hence, to illustrate the effect of these strain corrections on molecular conformations. For this purpose, we have used a linked atom least-squares (LALS) method.[16]

Correspondence to: R. Somashekar (rs@uomphysics.net).
Corresponding grant sponsor: Council of Scientific and Industrial Research.

Journal of Applied Polymer Science, Vol. 91, 3045–3053 (2004)

EXPERIMENTAL

Specimen preparation

The cocoon of *Bombyx mori* (Mysore, India) was degummed with 0.6% Marsciltes soap solution (300 ml) plus 0.3 g of sodium carbonate at 100°C for 0.5 h and was washed with hot, distilled water. This cocoon was again soaked in the above solution at 100°C for 1 h and washed with a large quantity of hot aqueous solution of sodium carbonate. This is associated with gradually changing its concentration from 0.3 to 0.1% and then washing with 0.2% acetic acid (1 L), and finally, washing by using hot, distilled water until no bubble was observed. This degummed cocoon was defatted with benzene and methanol solution (2/1 by volume) for 100 h in a Soxhlet extractor.

The silk fibroin (1 g) so prepared was dissolved in aqueous solution of 8*M* LiBr (20 ml). To remove LiBr salt, the solution was dialyzed against running water for 6 h and then renewed against distilled water every 3 h until no bromide ion was observed in the solution (usually more than 40 h). To make the fibroin concen-

tration of about 1%, distilled water (100 ml) was added to the dialyzed solution (20 ml). After being prepared at pH 7.8 by the phosphate buffer, the sample fibroin was digested by α-dry-motripsin (10 mg) with $CaCl_2$ (40 mg) in an incubator at 37°C for 24 h. The precipitate of C_p fraction (crystalline fraction of silk fibroin) was washed several times with distilled water. This was again defatted by a diethyl ether solution and then by a chloroform and methanol solution for 20 h for each. After washing several times with distilled water, the C_p fraction was lyophilized. Because the crystal form of the C_p fraction at this stage is usually the silk II modification, the specimen (0.3 g) was again dissolved in aqueous 8*M* LiBr solution (18 ml) at 37°C. After filtering the solution, distilled water (18 ml) was added and the solution was prepared at pH 4.2 by 10% acetic acid.[17] This solution was dialyzed against distilled water prepared at pH 4.2 for about 60 h at room temperature. After washing several times with distilled water, the precipitate was lyophilized.

Recording to X-ray diffraction pattern

By using nickel-filtered CuKα radiation from a microfocus X-ray generator (Rota Flex RU-200, Rigaku Co.) and in conjunction with a cylindrical camera, an X-ray diffraction pattern was obtained from powder specimens. This is shown in Figure 1. Previously reported cell parameters were used to index the observed reflections.[18] Intensities were obtained by microdensitometer scanning and were corrected for the Lorentz and polarization factors (LP).

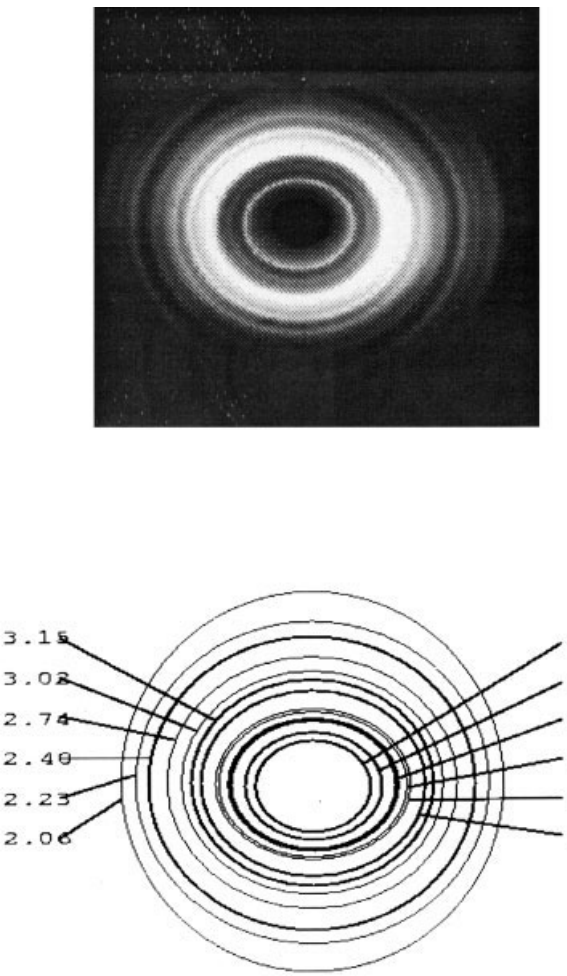

Figure 1 X-ray powder pattern from C_P fraction of *Bombyx mori* silk fibroin in silk I modification.

X-RAY PROFILE ANALYSIS

The crystal imperfection parameters such as crystal size ($\langle N \rangle$) and lattice strain (g) were determined by employing the Fourier method of Warren[19,20] and Hosemann's one-dimensional paracrystalline model,[21] wherein the simulated intensity profile was matched with an experimental one. The following equations were employed to compute the microstructural parameters.

The Warren's Fourier Method is as follows:

$$I(s) = \sum_{n=-\infty}^{\infty} A(n)\cos\{2\pi nd(s - s_0)\} \quad (1)$$

where $A(n)$ is the product of size coefficients $A_s(n)$ and lattice distortion (strain coefficient) $A_d(n)$. The expressions for $A_s(n)$ and $A_d(n)$ are given in refs. 19 and 20.

Hosemann's one-dimensional paracrystalline method states

$$I(s) = I_{N-1}(s) + I'_N(s) \quad (2)$$

where

$$I_N(s) = 2\ \mathrm{Re}\left[\frac{(1 - I^{N+1})}{(1 - I)} + \frac{Iv}{d(1 - I)^2}\{I^N(N(1 - I) + 1) - 1\}\right]^{-1} \quad (3)$$

Here, $v = 2ia^2s + d$ and $I = I_1(s) = \exp(-a^2s^2 + ids)$; $a^2 = \omega^2/2$. Also,

$$I'_N(s) = \frac{2a_N}{D(\pi)^{1/2}}\exp(iDs) \times [1 - a_N s\{2\mathcal{D}(a_N s) + i(\pi)^{1/2}\exp(-a_N^2 s^2)\}] \quad (4)$$

with $a_N^2 = \langle N \rangle \omega^2/2$, where ω is the standard deviation of the nearest neighbor probability function, $\mathcal{D}(a_N s)$ is the Dawson's integral or the error function with complex argument and can be computed. $\langle N \rangle$ is the number of unit cells counted in a direction perpendicular to the (hkl) Bragg plane, d is the spacing of the (hkl)

TABLE I
Crystal Size and Lattice Distortion (Residual Strain) Parameters in Silk I Modification

d in Å	(hkl)	$\langle N \rangle$	gin %	D_{surf} in Å
7.21	(020)	8.1 ± 0.4	7.9 ± 0.4	57.9 ± 2.9
5.61	(021)	35.8 ± 1.4	7.1 ± 0.8	196.8 ± 23.4
3.49	(002)	17.1 ± 0.9	7.5 ± 0.4	75.8 ± 3.9
3.94	(111)	31.0 ± 3.1	7.3 ± 0.7	121.4 ± 11.9
3.59	(121)	23.7 ± 3.8	7.1 ± 1.1	84.1 ± 13.5
2.94	(112)	31.8 ± 3.8	6.9 ±0.8	98.2 ± 11.8

Strain tensor components are $g_{11} = 0.043$; $g_{22} = 0.037$; $g_{33} = 0.039$; $g_{13} = 0.024$; $g_{32} = 0.035$; $g_{12} = 0.001$.

planes, Re refers to real part of the expression, s is sin θ/λ, λ being the wavelength of X-rays used, a is related to the standard deviation ω of lattice distribution function, and D is the crystal size ($=\langle N \rangle d_{hkl}$). $I'_N(s)$ is the modified intensity for the probability peak centered at D. The detailed procedure for the X-ray profile analysis is given in ref. 21. SIMPLEX, a multidimensional algorithm, is used for minimization. The averaged values of crystal imperfection parameters such as the crystal size $\langle N \rangle$ and the lattice distortion (the strain) g are given in Table I. One can simulate the intensity profiles by using these parameters and the above equations. Figure 2 shows the experimental and simulated intensity profiles of all the X-ray reflections observed in silk I modification.

The computation of the crystal size and lattice distortion was carried out for all six well-separated reflections and the results are given in Table I. The Fourier method of profile analysis is a quite reliable one as per the recent survey and results of Round Robin test. Essentially, the results given in Table I for a reflection (020) can be interpreted in the following manner. If one travels along the direction [020] through a distance of D_{surf}, then there is a lattice distortion of 8%. To put the results in a better perspective, we have projected these results onto a common plane X–Y by using the relation

$$\left(\frac{2}{N_{hkl}}\right)^2 = \left(\frac{\cos\theta}{Y}\right)^2 + \left(\frac{\sin\theta}{X}\right)^2 \tag{5}$$

and fitted the crystal size values of silk I into a shape-ellipsoid with one of the D_{surf} along the x-axis and Y_{min} has been obtained from iteration procedure by using the crystal size data of all other reflections observed in that particular sample (Table I). Here, θ is the angle between the two (hkl) planes and D_{surf} is the crystal size corresponding to the particular (020) reflection. Figure 3 shows the shape of the crystallite in silk I modification.

Computation of strain tensor components

The lattice distortions computed from different X-ray reflections can be used to calculate the six strain tensor components which will describe the paracrystallinity in silk I modification. For this purpose, we have employed the equation[22–24]

$$g^2_{(hkl)} = \frac{\sum_{i,k=1}^{3} \hat{h}_i^2 (\hat{h}_k / \hat{a}_k^2) g_{ki}^2}{\sum_{i,k=1}^{3} (\hat{h}_i^2 / \bar{a}_i^2)} \tag{6}$$

which relates the lattice distortion observed along any arbitrary direction to the six strain tensor components. Here $\hat{a}_i$ is the lattice parameters (a-, b-, c-axes), h_i's are Miller indices, convenient in the summation. By using the cell parameters and computed lattice strain values for various reflections, we have estimated the six strain tensor components corresponding to a unit cell in the case of silk I modification; these values are given in Table I. The trace of this symmetric tensor gives the fractional change in the volume of the unit cell due to residual strains. The off-diagonal elements give the fractional change in angles between the coordinate axes.

Strain corrected intensity profiles

Strain corrected profiles were generated by using the crystal size parameters along with the width of the crystal size distribution function and by employing equations (1), (2), (3), and (4) given earlier in this article. Strain-corrected integrated intensities of the profiles were used for constructing a molecular model which could explain the observed X-ray intensity data. Figure 4 shows both experimental and strain corrected X-ray intensity profile for the (020) reflection.

Molecular modeling

To find the effect of residual strain corrections on the intensity profiles and hence on the molecular and crystal structure of silk I modification, we started with a hexapeptide, L-Ala-Gly-L-Ala-Gly-L-Ser-Gly, as a chemical repeating unit of the C_p fraction for the analysis. Molecular models having the appropriate helical symmetry and fiber repeating period were generated using LALS description with all bond lengths and angles held constant, which are shown in Figure 5. The molecular structure of the silk fibroin has a 2/1-helical symmetry. That is, two chemical repeating units of L-Ala-Gly are constant fiber repeating period. The value of dihedral angles (ϕ, ψ) of Glycine and Alanine residues were taken from the results of our earlier investigation.[6] The molecular conformation satisfies both sterical and mathematical requirements, as (ϕ, ψ) values are within the allowed region of (ϕ, ψ) map for

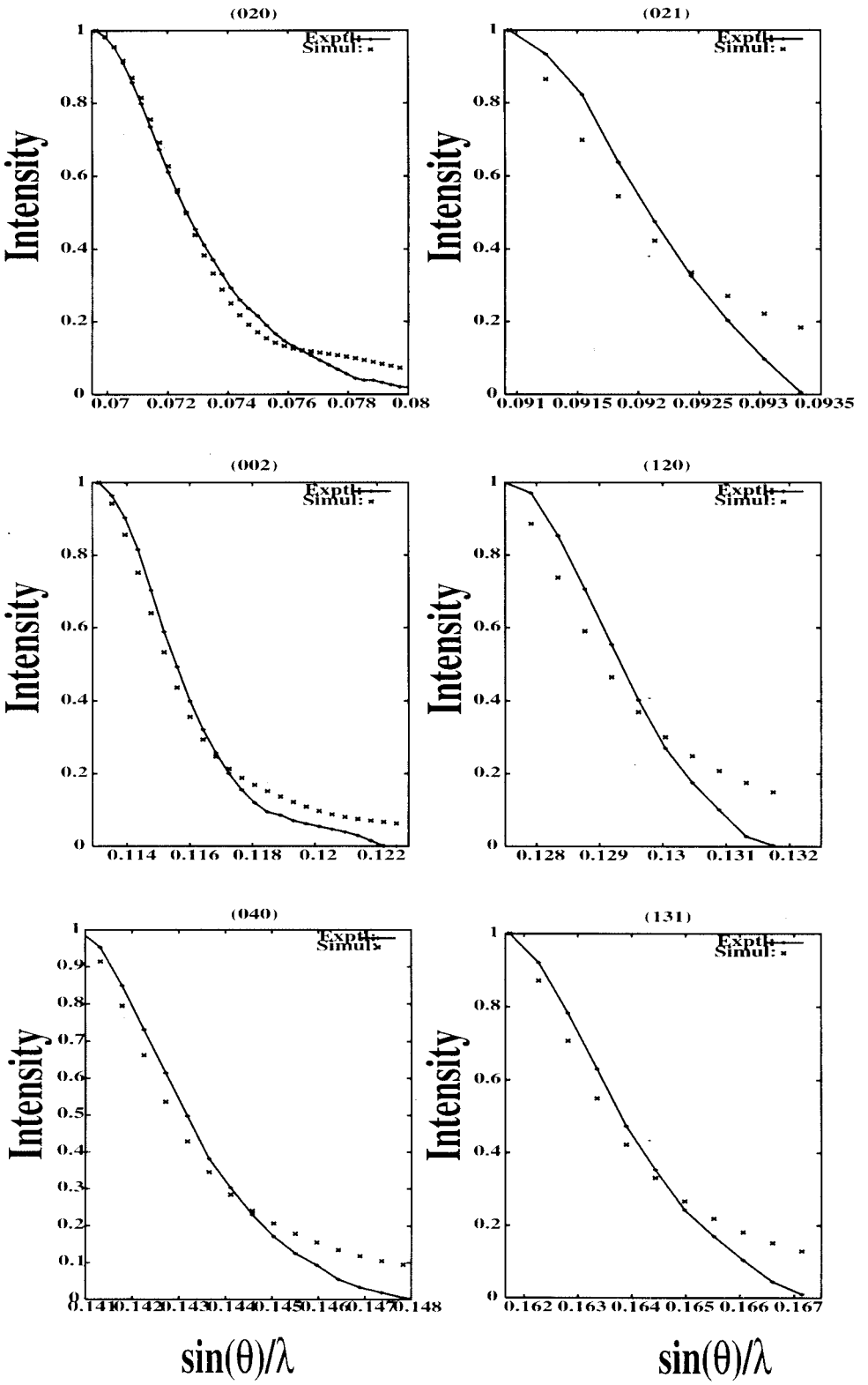

Figure 2 Experimental and simulated X-ray intensity profiles of various reflections observed in silk I.

the Alanine residue. These values are in the *Bridge* and the fourth quadrant regions of the Ramachandran map, respectively. In the following section, the most plausible space group and the number of chemical repeating unit of L-Ala-Gly in a unit cell were determined to be $P2_12_12_1$ and four ($\tau = 4$), respectively. To pack four chemical repeating units in a unit cell, the 2_1- helical units of the molecule must coincide with the

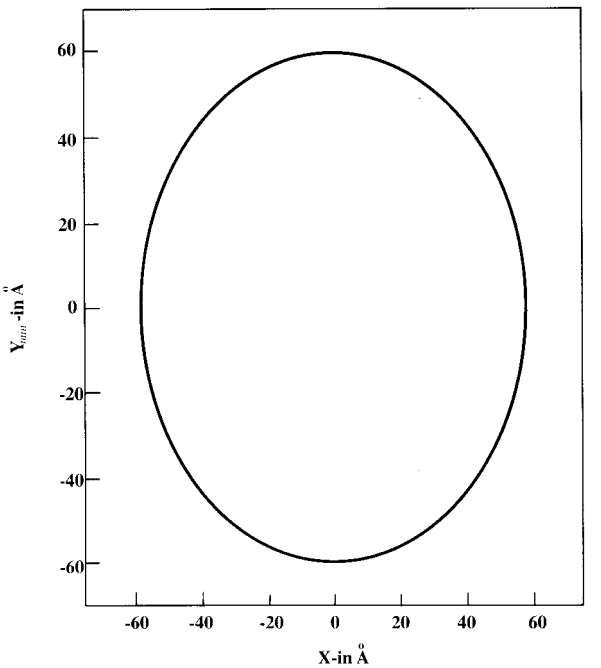

Figure 3 Shape and size of crystallite in silk I modification.

crystallographic 2_1-axis parallel to the *c* direction. For positioning the molecular model in the unit cell, two additional parameters were used to define the relative axial rotation (μ) and translation (w) along the *c*-axis. To obtain the appropriate values for each packing model, μ and w were systematically changed by 20° intervals from 0 to 180° and 0.05 intervals from 0 to 0.5, respectively. At each stage in the modeling and

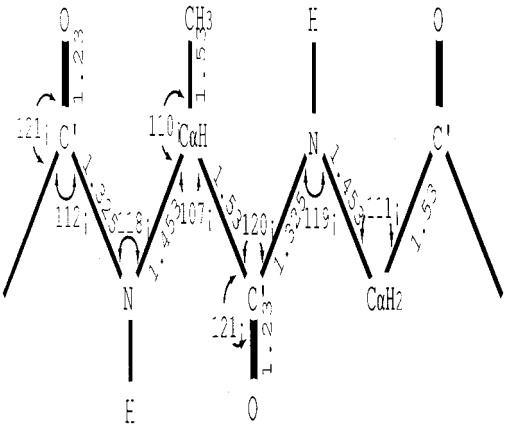

Figure 5 The values of bond lengths (Å) and angles (°) used in the molecular model building.

refinement of the structure, we sought to minimize the quantity Ω in the following least-squares fashion:

$$\Omega = \Sigma w(|F_0| - |F_c|)^2 + S\Sigma_j \epsilon_j + \Sigma_h \lambda_h G_h \qquad (7)$$

The first summation in Ω ensures the optimum agreement between the observed (F_o) and the calculated (F_c) X-ray structure amplitudes. w is the weight of each reflection. The second term ensures the optimization of noncovalent interatomic interactions (ϵ_j). S is the scale factor used to adjust the overall weight of the second term with respect to the first. The third imposes, by the method of Lagrange undetermined multipliers (λ_h), the exact constraints (G_h) which we have chosen.

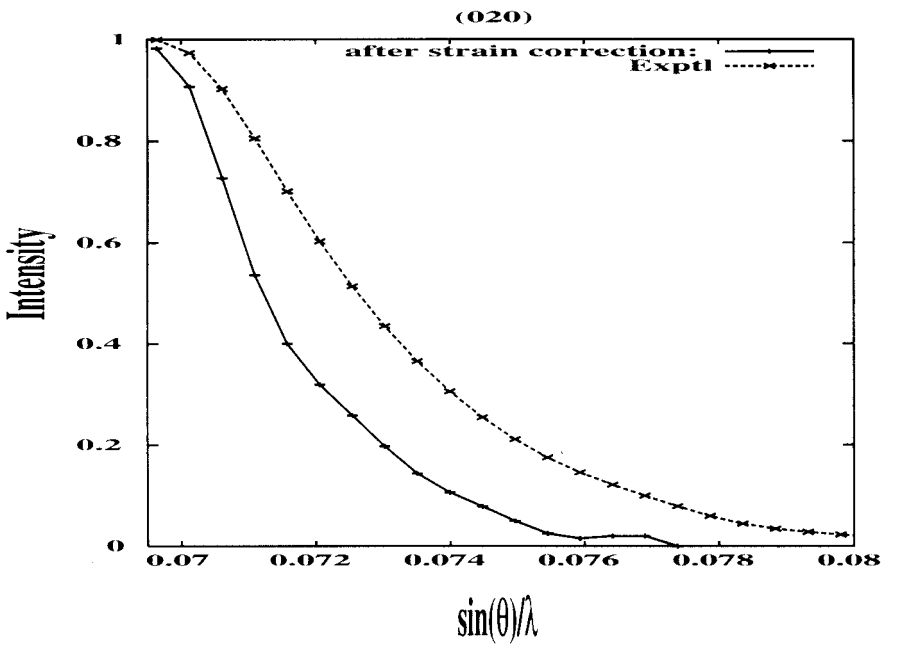

Figure 4 Experimental and strain-corrected X-ray intensity profiles of (020) reflection in silk I.

Atomic scattering factors for calculating structure factors were obtained by using the method and values given in International Tables for X-ray Crystallography.[25] Computations were carried out on an IBM PC.

Structure determination after correcting for residual strains

Among the total of 12 observed reflections (Fig. 2), we have carried out residual strain corrections for six well-separated prominent reflections, and the corresponding integrated intensities were used as the input to LALS program. The reflections below the observational threshold were also included in the structure analysis. That is, unobserved reflections within 2.0 Å resolution were assumed to have half of the intensity of the observational threshold. The cell parameters are $a = 4.65$, $b = 14.24$, and $c = 8.88$ Å. The space group is $P2_12_12_1$. The calculated and experimental densities are 1.39 and 1.49 g/mL. In structure refinement, we have minimized

$$R = \frac{\Sigma|F_o| - |F_c|}{\Sigma|F_o|} \tag{8}$$

$$R_w = \frac{\Sigma_w(|F_o| - |F_c|)^2}{\Sigma w F_o^2} \tag{9}$$

In this study, the weight of each reflection w was fixed at 1.0.

RESULTS AND DISCUSSION

Figure 2(a–f) shows the experimental and simulated X-ray intensity profiles using the parameters given in Table I and eqs. (1), (2), (3), and (4). It is evident from these figures and the goodness of fit that the microstructural parameters are quite reliable. Also, it would not be out of place to mention here the views of Round Robin test wherein it was observed that the Fourier method of profile analysis gave quite reliable values. The shape of crystallite computed from these microstructural data and projected on a plane is shown in Figure 3, which indicates an ellipsoidal shape similar to the shape observed in silk II modification. In fact, the observed crystal size distribution along different directions follow a log-normal behavior. The lattice strain given in Table I physically represents the percentage of lattice disorder that one finds in silk I modification at the periphery of the crystallite region given in Figure 3. The degrees of strain per unit cell are the strain tensor components and they are given in Table I.

Effect of strain corrected intensity data on the molecular configuration

The molecular conformation of silk I is one of the important structures of biopolymers that has been determined with clarity.[3] Okuyama et al.[6] have reported crystal structure of silk I modification by using 12 observed X-ray diffraction intensities and 9 unobserved (below threshold) diffraction intensities up to 2.0 Å resolution. In the present study, with better integrated intensities of broadened X-ray Bragg reflections, we observe the same molecular conformation, which looks like a Crank-Shaft, as proposed by Lotz and Keith[3,6] for model peptide of silk fibroin. Figure 6(a,b, and c) shows the crystal structure of silk I modification with and without residual strains when viewed along *a*-, *b*-, and *c*-directions. The refinement calculations were carried out with hexapeptide repeating unit $(L\text{-Ala-Gly})_2$-L-Ser-Gly. Refined structure with residual strain-corrected intensity after several cycles is summarized in Table II, along with those of earlier results wherein such a correction was not incorporated. A comparison reveals that the dihedral angles were changed only by several degrees and significant conformational changes were not observed in the present case. Here also, we observe the N—H $\cdots$ O and O—H $\cdots$ O type of hydrogen bonds. By including the residual strain correction for the integrated intensities, we observe slight increase in R and R_w values. Our main aim of including these strain corrections was to find out the molecular conformational changes due to the residual strains, and hence, to identify the reason for mechanical instability of silk I modification. Atomic coordinates of the chemical repeating unit are listed in Table III and its packing structures are shown in Figure 6. In Figure 6, the present packing structure is compared with the one obtained without incorporating the residual strain corrections for the integrated intensities (shown in the background). The torsion angles (ϕ, ψ) in L-Ala- are in the *Bridge* region, which were intermediate between L_R and β and (ϕ, ψ) in Gly- lie in the fourth quadrant of Ramachandran's Map.[26] The *Bridge* region is the region where quite a large number of amino acid residues were found in the protein structures. The values of these torsion angles vary significantly after using the residual strain corrected integrated intensity data. Although there is not much change in the conformation of the molecules when seen down the *a*- and *b*-axes, there seems to be significant change in the molecular arrangement in the *ab*- plane. The residual strains present in silk I modification seem to alter the molecular conformation in the (*a*–*b*) plane and hence may enhance the fragility of the silk I modification, which results in easier transition to silk II modification, despite reasonable hydrogen bond network (see Table II). Contact σ, which represents the stereochem-

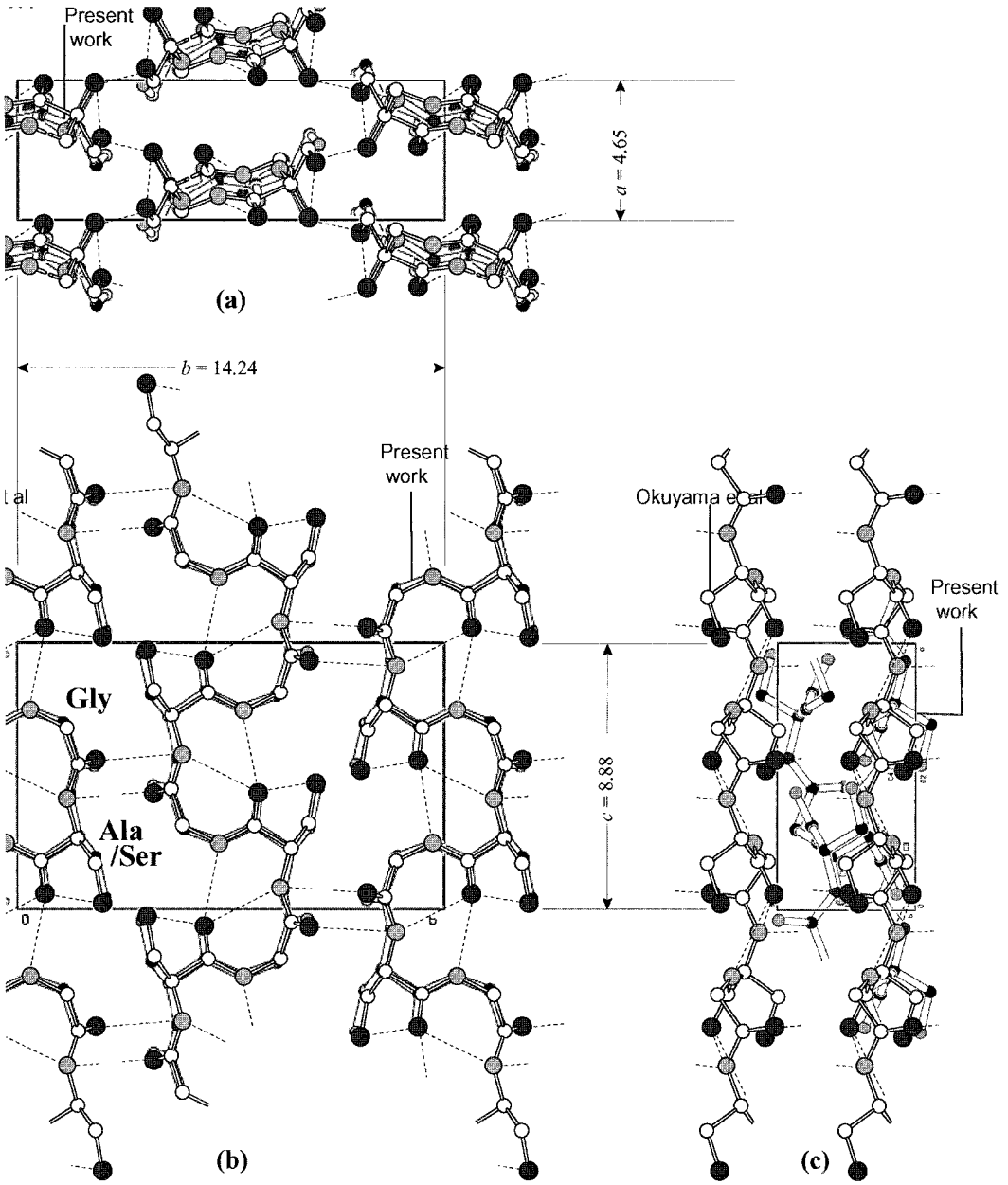

Figure 6 Crystal structure of silk I with and without strain corrections.

ical energy of the final structure with $P2_12_12_1$ space group, has a better low value in the present case when compared to the earlier results. The reason for the observed increase in the goodness-of-fit parameters even after using the strain-corrected intensities may be due to the fact that we have not been able to incorporate the observed fractional changes in the volume and angles between the axes of the unit cell.

CONCLUSION

Wide-angle X-ray scattering studies of silk I modification show that there are broadening of X-ray reflections due to Hosemann's paracrystalline-like disorder. By using a model developed by us on the basis of Warren's Fourier method, we have estimated the crystal size and lattice distortion (residual strain) present in this modification along different directions. We have computed the shape and size of the crystallite, residual strain tensor components and then analyzed the impact of such residual strains on the molecular conformations. The changes in crystal structure have been quantified in terms of crystal packing parameters. An important aspect of this investigation is the use of X-ray powder data for structure analysis by using linked atom least-squares method.

TABLE II
Refinement Parameters for Silk I with (Ala-Gly)$_2$-Ser-Gly Repeating Unit

Refined parameters	Without strain corrections	After correcting for the residual strain
Torsional angle (°)		
$\phi_{\text{Ala-Ser}}$	−112.09	−101.71
$\psi_{\text{Ala-Ser}}$	−5.55	−12.15
$\omega_{\text{Ala-Ser}}$	179.23	160.94
χ_{Ser}	174.64	167.85
ϕ_{Gly}	71.39	73.83
ψ_{Gly}	−98.66	−105.87
ω_{Gly}	−172.10	177.03
Eulerian angle (°)		
ϵ_x	14.50	0.23
ϵ_y	52.34	62.36
ϵ_z	−62.10	−49.15
Other parameters		
$S(\AA)$	−2.0077	−2.0073
μ(°)	90.29	90.27
w	0.0464	0.0464
Scale factor	1.506	2.200
Attenuation factor	5.676	−0.1509
Hydrogen bonds, intermolecular between antiparallel chains, distance (Å), angle (°), intramolecular	N_1(Ala) . . . O2(Gly) (2.98, 76.90) N2(Gly) . . . O1(Ala) (3.13, 125.6) N1(Ala) . . . O1(Ala) (2.88, 86.4) O2(Ser) . . . O1(Ala) (2.65, 88.5)	N1(Ala) . . . O2(Gly) (2.85, 79.87) N2(Gly) . . . O1(Ala) (2.87, 127.72) N1(Ala) . . . O1 (2.96, 79.95) O3(ser) . . . O1(Ala) (2.73, 86.83)
R-factors Including unobserved reflections		
Including unobserved reflections		
R_c	0.069	0.178
R_w	0.082	0.186
Excluding unobserved reflections		
R_c	0.068	0.179
R_w	0.079	0.186

TABLE III
Fractional Atomic Coordinates of Silk I with the Repeating Unit of (Ala-Gly)$_2$-Ser-Gly after Incorporating the Residual Strain Corrections in the Integrated Intensities of X-ray Reflections

Atoms	*x*	*y*	*z*
Ala			
N1	0.421	0.123	0.431
HN1	0.615	0.093	0.442
C1(α)	0.347	0.144	0.276
C5(β)	0.610	0.184	0.195
HC1	0.187	0.190	0.277
C2(′)	0.249	0.058	0.185
O1	0.135	0.068	0.061
Gly			
N2	0.292	−0.025	0.248
HN2	0.432	−0.037	0.331
C3(α)	0.136	−0.109	0.199
HC31	−0.073	−0.094	0.189
HC32	0.162	−0.160	0.275
C4(′)	0.252	−0.141	0.046
O2	0.013	0.180	0.537
Ser			
O3	0.539	0.206	0.043

One of the authors (R.S.) acknowledges the financial support of Council of Scientific and Industrial Research (CSIR), New Delhi.

References

1. Shimizu, M. Bull Imp Sericult Expt Sta Jpn 1941, 10, 475.
2. Lotz, B.; Cesari, G. C. Biochimie 1970, 61, 205.
3. Lotz, B.; Keith, H. D. J Mol Biol 1971, 61, 201.
4. Valluzzi, R.; Gido, S. P. Biopolymers 1997, 42, 705.
5. Marsh, R. E.; Corey, R. B.; Pauling, L. Biochim Biophys Acta 1955, 16, 1.
6. Okuyama, K.; Somashekar, R.; Noguchi, K.; Ichimura, S. Biopolymers 2001, 59, 310.
7. Gopalkrishne Urs, R.; Subramanyam, G.; Somashekar, R. Textile Res J 1993, 63, 610.
8. Somashekar, R.; Gopalkrishne Urs, R. J Appl Polym Sci 1993, 50, 949.
9. Somashekar, R.; Gopalkrishne Urs, R. Pramana, . J Phys 1993, 40, 335.
10. Somashekar, R.; Somashekarappa, H.; Subramanyam, G.; Prahllad U. D. Eur Polym J 1997, 33, 963.
11. Somashekarappa, H.; Nadiger, G. S.; Somashekar, T. H.; Prabhu, J.; Somashekar, R. Polymer 1998, 39, 209.
12. Annadurai, V.; Subramanyam, G.; Gopalkrishne Urs, R.; Somashekar, R. J Appl Polym Sci 2001, 79, 1979.

13. Baldev, R.; Annadurai, V.; Somashekar, R.; Madan, R.; Siddaramaiah, 53. Eur Polym J 2001, 37, 943.
14. Warren, B. E.; Averbach, B. L. J Appl Phys 1950, 21, 595.
15. Warren, B. E. Acta Cryst 1955, 8, 483.
16. Smith, P. J. C.; Arnott, S. Acta Crystallogr 1978, A34, 3.
17. Nakajima, Y.; Takanashi, K.; Okuyama, K.; Hirabayashi, K. J Phys Chem 1975, 56, 83.
18. Okuyama, K.; Takanashi, K.; Nakajima, Y.; Hasegawa, Y.; Hirabayashi, K.; Nishi, N. J Seric Sci Jpn 1988, 57, 23.
19. Somashekar, R.; Hall, I. H.; Carr, P. D. J Appl Crystallogr 1989, 22, 363.
20. Hall, I. H.; Somashekar, R. J Appl Crystallogr 1991, 24, 1051.
21. Somashekar, R.; Somashekarappa, H. J Appl Cryst 1997, 30, 147.
22. Wilke, W.; Martis, K. W. Colloid Polym Sci 1974, 252, 718.
23. Martis, K. W.; Wilke, W. Progr Colloid Polym Sci 1977, 62, 44.
24. Hein, K. M.; Haberle, K. D.; Wilke, W. Colloid Polym Sci 1991, 269, 675.
25. Kasper, J. S.; Lonsdale, K., Eds. International Table for Crystallography: Kynoch Press: Birmingham, 1974; Vol. 4; p 71.
26. Ramachandran, G. N.; Ramakrishnan, C.; Sasisekharan, V. J Mol Biol 1963, 7, 95.